Virchows Arch (1995) 426:577–586

ORIGINAL ARTICLE

Jun Cheng · Tarou Irié · Ryuichi Munakata
Shin Kimura · Hiroaki Nakamura · Rong-Gen He
Ai-Ru Liu · Takashi Saku

Biosynthesis of basement membrane molecules by salivary adenoid cystic carcinoma cells: an immunofluorescence and confocal microscopic study

Received: 13 December 1994 / Accepted: 28 March 1995

Abstract The biosynthesis of basement membrane molecules and fibronectin was studied in vitro in the two different human cell systems (ACC2 and ACC3) established from adenoid cystic carcinomas (ACC) of the salivary gland using immunofluorescence and confocal microscopy. When the cells were attached and spread on dishes, fine granular immunofluorescence for type IV collagen, laminin, heparan sulphate proteoglycan, entactin, and fibronectin first appeared diffusely in the cytoplasm, and then changed into aggregation of coarse granules in the perinuclear area. With formation of colonies, these signals were present in the extracellular space, initially in the basal aspect of attached cells and consequently in the lateral intercellular space. After the cells formed a confluent monolayer, extracellular signals started to decrease in inverse proportion to the reappearance of intracellular ones. The results indicate that the parenchymal cells of ACC synthesize these five extracellular matrix molecules, secrete them into the extracellular milieu and remodel the extracellular deposits. It is suggested that the characteristic stromal architecture of ACC, represented by stromal pseudocysts, results from their own secretion of the basement membrane molecules and fibronectin.

J. Cheng · T. Irié · R. Munakata · S. Kimura · T. Saku (✉)
Department of Pathology, Niigata University School of Dentistry, 2-5274 Gakkocho-dori, Niigata 951, Japan

R. Munakata
Department of Oral and Maxillofacial Surgery, Niigata University School of Dentistry, Niigata, Japan

H. Nakamura
Department of Oral Anatomy, Niigata University School of Dentistry, Niigata, Japan

R.-G. He
Department of Oral Maxillofacial Surgery, School of Stomatology, Shanghai Second Medical University, Shanghai, China

A.-R. Liu
Department of Oral Pathology, School of Stomatology, Shanghai Second Medical University, Shanghai, China

Key words Basement membranes · Adenoid cystic carcinoma · Extracellular matrix · Immunofluorescence · Confocal laser microscopy

Introduction

Adenoid cystic carcinoma (ACC) arising in the human salivary gland is characterized histopathologically by cribriform structures which consist of two types of luminal structures: one consists of stromal pseudocysts surrounded by myoepithelioid cells and the other is composed of ductal mimics containing salivary material in their lumina [4, 8, 19, 23, 30]. Previous immunohistochemical studies using surgical material have shown that the stroma of ACC including the pseudocystic space contains basement membrane molecules: type IV collagen, laminin, heparan sulphate proteoglycan and entactin [1, 6, 10, 32, 33]. Since the pseudocystic space contains no cellular component but is surrounded by tumour cells, it has been assumed that the extracellular matrix retained in the space has been produced by the parenchymal cells [8, 10, 23]. Further, frequent invasion along peripheral nervous tissues or haematogenous metastasis seen in this tumour may relate to the affinity of the cells for basement membranes, as vascular vessels and peripheral nerves are rich in basement membranes [10].

Morphological evidence indicates that the pseudocystic structures result from an excessive basal secretion and retention of extracellular matrix produced by the tumour cells [7, 9, 14, 15, 29]. However, it is unknown whether the characteristic stroma of ACC is produced by the parenchymal cells or by stromal cells.

In this study, we sought to confirm that these basement membrane molecules in the stroma are produced by the parenchymal cells themselves. To this end, we used two cell systems, ACC2 and ACC3, independently established from the human ACC [13]. We determined the biosynthesis of the four basement membrane molecules and fibronectin immunohistochemically in vitro.

Materials and methods

Two cell systems, ACC2 and ACC3 were established from ACC arising in a palatal minor salivary gland of a 28-year-old woman and in the parotid gland of a 49-year-old man, respectively [13]. The cells were cultured in RPMI-1640 medium (Nissui, Tokyo, Japan) containing 15% fetal calf serum (Gibco-Life Technologies, Gaithersburg, Md., USA), 1% glutamine, 50 μg/ml streptomycin and 50 IU/ml penicillin, and incubated at 37° C in humidified 5% carbon dioxide/95% air atmosphere. For this experiment, the ACC2 and ACC3 cells between the 150 and 170 passages were used.

All the primary antibodies used in this study were polyclonal antibodies raised in rabbits against four basement membrane molecules: human type IV collagen, human laminin (P1 fragment), mouse heparan sulphate proteoglycan (core protein) and mouse entactin as described elsewhere [10]. Fibronectin was purified from human plasma by the method of Engvall et al. [11] and the antiserum was raised in rabbits. These polyclonal antibodies were purified by passage through columns of antigen-coupled Sepharose-4B (Pharmacia, Uppsala, Sweden). In immunohistochemical experiments, the antibodies were used at protein concentrations of 10–50 μg/ml. The second antibodies were rhodamine-conjugated goat anti-rabbit IgG (1:50, Miles Scientific, Naperville, Ill., USA).

ACC2 and ACC3 cells at a concentration of 3×10^6 in 0.1 ml culture medium were injected subcutaneously in the back of three each of male BALB/c (nu/nu) mice, 4 weeks of age. The animals were housed in clean boxes in a sanitary and ventilated animal room and maintained under constant conditions (22° C, 12 h light/dark cycle) with free access to sterilized solid food and autoclaved water. With the animals under ether anaesthesia, the transplanted tumour masses were excised, fixed in 95% ethanol overnight at 4° C and embedded in paraffin. Serial sections cut from paraffin blocks were utilized for histological examination with haematoxylin and eosin, toluidine blue, alcian blue (pH 2.5, 1.0 and 0.5) stainings, periodic acid Schiff (PAS), and the peroxidase-antiperoxidase immunostainings with antibodies described above.

The growth rates of ACC2 and ACC3 were determined by enumeration of cell nuclei from the replicate culture method [17]. The cells were seeded at cell concentration of 3×10^4 in 1 ml complete medium in a 2 ml plastic tube with a screw cap, fed every 2 days with fresh medium, and incubated at 37° C in an airtight condition. The cell numbers were counted for three sets of tubes every 24 h for 10 days. In order to examine the effect of extracellular matrix on the growth of ACC cells, another set of plastic tubes were coated with fibronectin at concentration of 30 μg/ml in 0.05 M TRIS-hydrochloric acid (pH 7.4) for 24 h at 4° C prior to seeding the cells. Fibronectin was prepared from the human plasma as described above. Student's *t*-test was used for statistical analysis.

For *immunohistochemistry*, the cells, at concentration of 3×10^4, were plated onto a 35 mm plastic dish in which a piece of cover glass was placed. The dishes were fixed with 4% paraformaldehyde in 0.1 M phosphate buffer (pH 7.4) for 30 min on ice every 24 h for 10 days after plating, and then permeabilized by adding with 0.2% Triton X-100 into the fixative for 20 min on ice. After overnight treatment with 5% milk protein in phosphate buffered saline (PBS; pH 7.4) containing 0.05% Triton X-100 to prevent non-specific protein binding, the dishes were stained with an indirect immunofluorescence technique. They were incubated with the primary and secondary antibodies for 1 h each at room temperature. Each dish was divided into six compartments with rubber cement, to perform six different immunostainings, including a control experiment, simultaneously. After immunostaining, cover glasses were removed from the dishes and mounted on slide glasses with 90% glycerol in PBS. As controls, nonimmune rabbit IgG was used of specific primary antibodies. The slides were examined in a phase contrast microscope equipped with epifluorescence optics and an automatic camera system (Olympus BH-2, PM10AD, Tokyo, Japan). Representative slides were photographed on Fujichrome 400 film.

Confocal microscopy was carried out on immunostained sections using a laser scanning microscope (Olympus LSM-GB200). An argon ion laser operating at 515 nm was used as the excitation source. The scan time was 10 s per frame. Ten-to-twenty frames 0.8 μm or 1 μm each in Z-axis from the bottom to the surface of a fixed cell layer were scanned for each antibody. Confocal images saved in a personal computer (Hewlett Packard Vectra 386/25) were photographed by using a film recorder (Avio FR-3000, Tokyo, Japan) and Kodak T-Max film.

Results

Transplanted tumor

After 2–4 weeks of injection of transplanted ACC2 and ACC3 cells, subcutaneous tumour masses of 5–20 mm in diameter were formed in the backs of BALB/c (nu/nu) mice. On cut section of surgically removed tissues, the tumours were well encapsulated with a smooth and thin layer of fibrous tissue and were greyish white in colour. Histologically, there were numbers of pseudocysts in the tumour nests (Fig. 1a). The cystic contents were PAS/alcian blue-positive and showed metachromasia with toluidine blue staining (Fig. 1b). Furthermore, these cystic spaces were immunopositive for fibronectin and the four basement membrane molecules (Fig. 1c). ACC2 and ACC3 cells were shown to preserve the ability to form pseudocystic structures, the basic characteristic of ACC.

Cell growth

As shown in Figure 2, the doubling time of ACC3 cells was about 36 h. On the second day after plating, ACC3 cells started logarithmic growth and entered their stationary phase after day 6. The maximum cell number, 4.5×10^5, 15 times the initial number of cells plated, was obtained at day 9, thereafter ACC3 cells decreased in number. When seeded in tubes precoated with fibronectin, the doubling time of ACC3 cells became much shorter (16 h), and they increased in number up to 20 times at day 9. The difference between the two conditions was statistically significant through the experimental period ($P<0.01$), especially from days 2–7 ($P<0.001$). ACC2 cells showed almost the same growth pattern (data not shown). The results indicate that ACC2 and ACC3 cells proliferated more in the presence of fibronectin.

Immunohistochemical study

ACC2 and ACC3 cells were shown to produce at least four basement membrane molecules: type IV collagen, laminin, heparan sulphate proteoglycan and entactin in addition to fibronectin. Since there was no distinct difference in the staining patterns between ACC2 and ACC3 cells, we describe the results of immunofluorescence without distinguishing the two in the following.

On the first day after seeding, diffuse or fine granular signals for these molecules were seen in the cytoplasm.

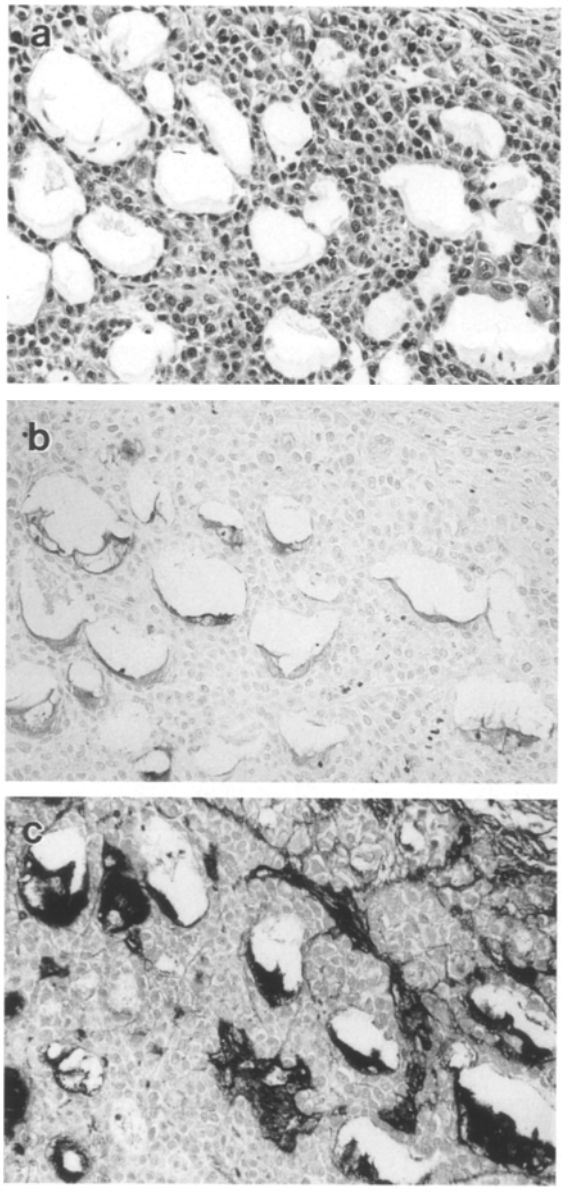

Fig. 1a–c Histology of transplanted tumour of ACC3 cells. **a** Haematoxylin and eosin, **b** alcian blue stain (pH 2.5) and **c** immunoperoxidase stain for heparan sulphate proteoglycan (HSPG), ×150. Pseudocystic spaces stain positive for alcian blue and basement membrane molecules

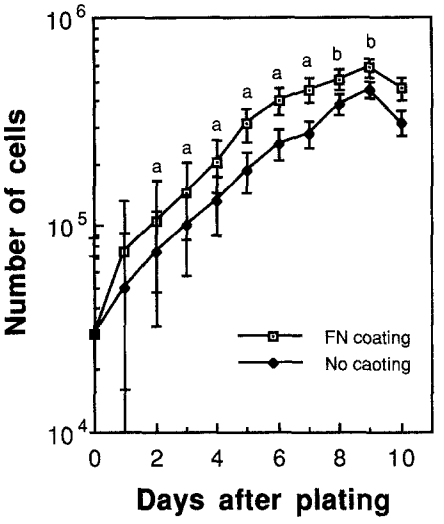

Fig. 2 Growth curve of ACC3 cells with (⊡) or without (◆) the presence of fibronectin (*FN*), measured by replicated culture method. Significant difference from value for absence of fibronectin by Student's *t*-test ([a] $P<0.01$, [b] $P<0.001$)

We called this appearance the "endopasmic reticulum (ER) pattern". Then, they became condensed into the perinuclear area, which we called the "Golgi pattern". Soon after the Golgi pattern appeared, the staining changed into punctate or short-linear structures in the intercellular spaces whereas intracellular signals disappeared. The intermittent extracellular fluorescence became continuous, resulting in a honeycomb-like meshwork around individual cells. Then, extracellular deposits of these molecules became thicker over the cellular areas. After confluence, the thick extracellular staining started to decrease and intracellular signals re-emerged. Such a continual change in the immunostaining pattern was consistent irrespective of the molecules examined, although there were minor variations. In the following, we will describe the details.

Type IV collagen

An intracellular fluorescence signal for type IV collagen was initially observed 24 h after plating. The staining was diffuse and finely granular (Fig. 3a). From day 2 to day 4, the granular staining greatly increased in size, number and intensity (Fig. 3b). We interpreted these signals as type IV collagen biosynthesized in the rough ER (rER), so that we called this type of staining the ER pattern. At day 5, the predominant feature was aggregation of intracellular signals in the perinuclear area. This was interpreted as transport of type IV collagen molecules into the Golgi apparatus; the Golgi pattern (Fig. 3c). At day 6, finely dotted or thread-like staining appeared in the extracellular space for the first time (Fig. 3d). This was regarded as intercellular deposition of type IV collagen secreted from the cells. Figure 3e shows advanced extracellular accumulation of type IV collagen after day 7. When the extracellular deposits were conspicuous over ACC cell colonies, the intracellular staining became indiscernible. The cells reached confluence by day 8. Thereafter, cell nests with ER/Golgi patterns frequently re-appeared, whereas their extracellular signals became less intensive (Fig. 3f).

Laminin

The ER pattern for laminin was seen at day 1 (Fig. 4a). Then, intracellular signals became larger and more intense at the periphery of cells (Fig. 4b). The Golgi pat-

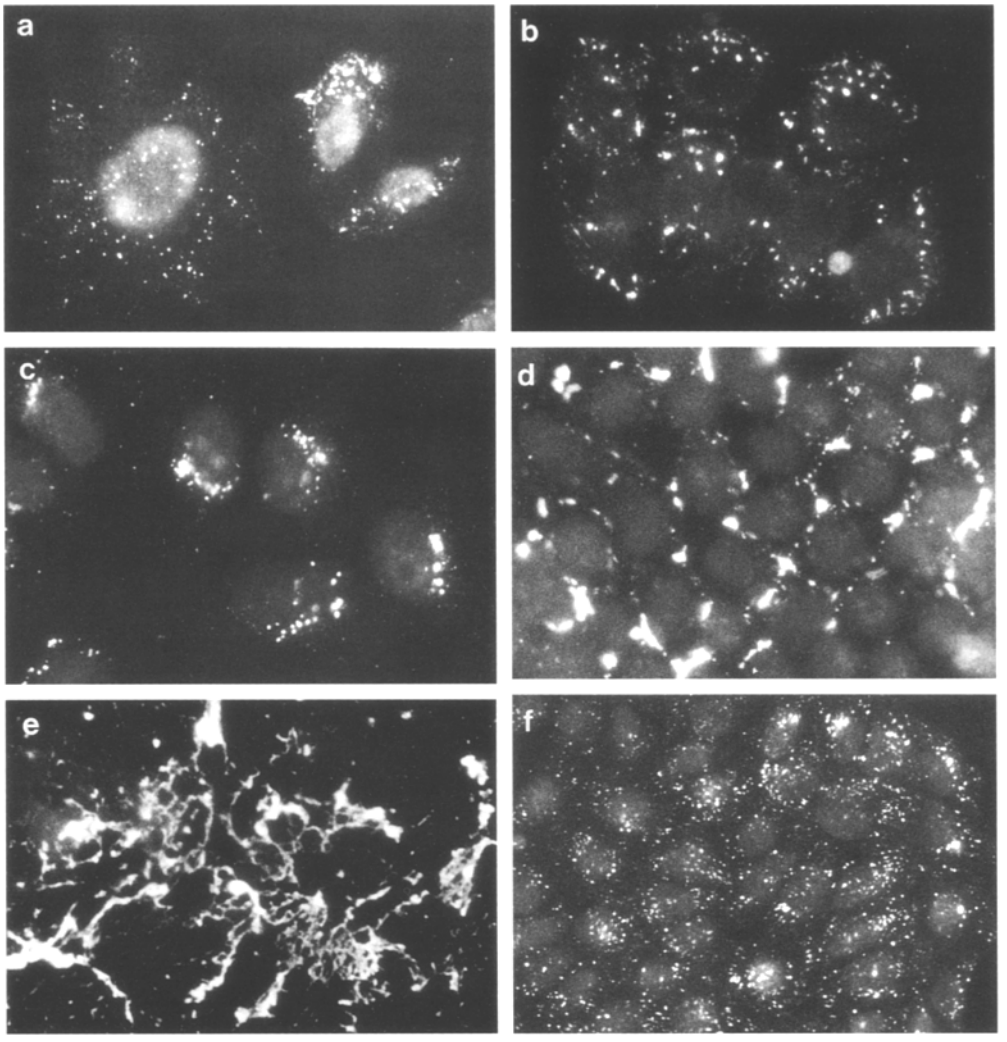

Fig. 3a–f Immunofluorescence for type IV collagen in ACC3 cells. **a** Day 1, ×400. **b** Day 3, ×480. **c** Day 5, ×480. **d** Day 6, ×480. **e** Day 7, ×560. **f** Day 8, ×200. Signals of endoplasmic reticulum (ER; **a**, **b**) and Golgi patterns (**c**) change into extracellular dots (**d**) or meshes (**e**). Intracellular signals reappear with decrease of extracellular ones at a later stage (**f**)

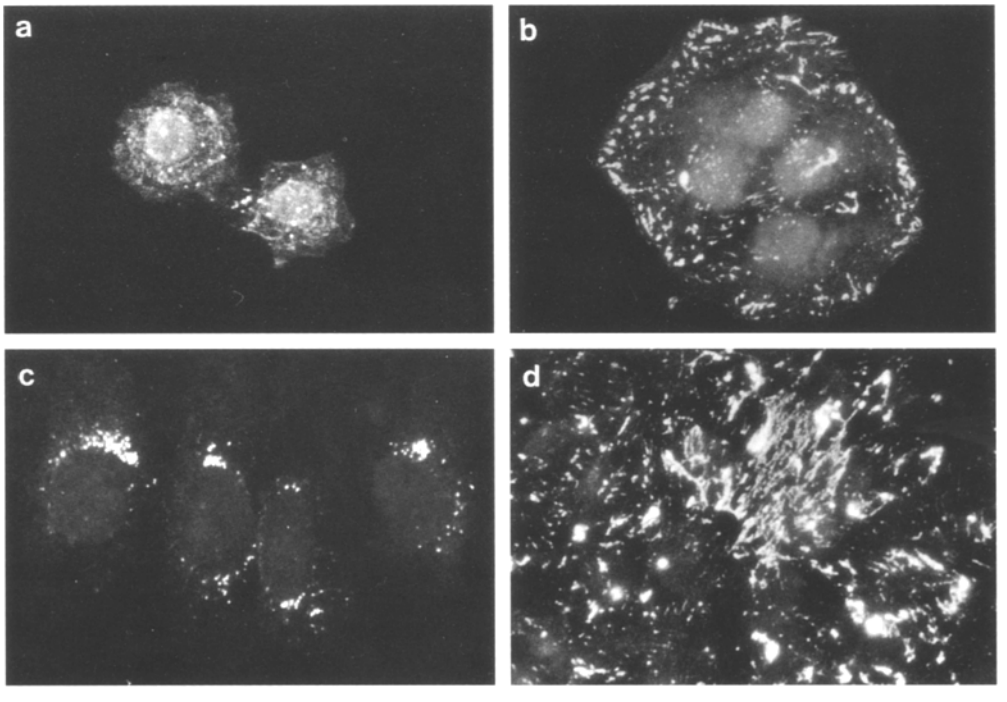

Fig. 4a–d Immunofluorescence for laminin in ACC3 cells. **a** Day 1, ×400. **b** Day 3, ×400. **c** Day 5, ×560. **d** Day 6, ×400. ER (**a**, **b**), Golgi patterns (**c**) and web of extracellular deposits (**d**) are clearly distinguished

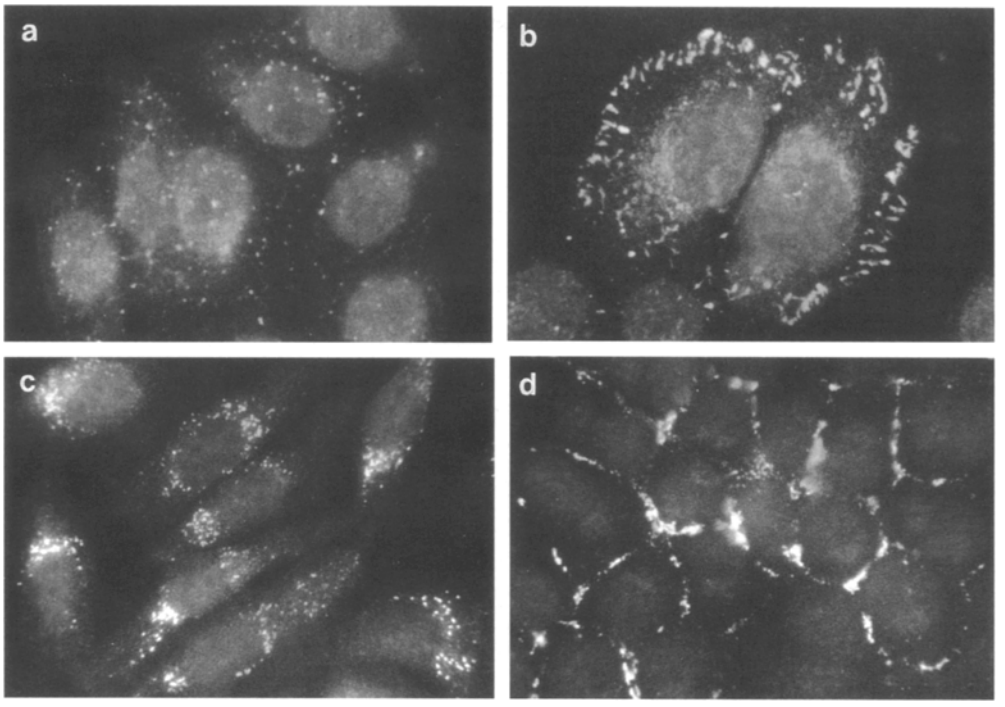

Fig. 5a–d Immunofluorescence for HSPG in ACC3 cells. **a** Day 1, ×560. **b** Day 2, ×560. **c** Day 5, ×480. **d** Day 7, ×560. ER (**a**, **b**) and Golgi patterns (**c**) and meshworks in intercellular space (**d**) are obviously recognized

tern first appeared earlier than that of type IV collagen at day 4, and increased in number and intensity at day 5 (Fig. 4c). The Golgi pattern of laminin was more intense than any other extracellular molecules examined. At day 6, extracellular signals started to appear and haphazard deposits were noticeable (Fig. 4d). From the eighth day after plating, ER and Golgi patterns were shown up again with decreased extracellular staining.

Heparan sulphate proteoglycan

Immunostaining patterns for heparan sulphate proteoglycan were quite similar to those of type IV collagen. ER pattern was seen at day 1 (Fig. 5a) and staining intensity gradually increased with time (Fig. 5d). At the fifth day after plating, the Golgi pattern was emerging (Fig. 5c). Punctate signals were characteristic of heparan sulphate proteoglycan. From the sixth day after plating, the extracellular signals were increased, while intracellular ones decreased (Fig. 5d). After day 9, ER and Golgi patterns returned.

Entactin

Immunofluorescence for entactin was not so evident as that of the other molecules examined. Its ER pattern with a small number of granula signals was observed from day 1 to day 5 (Fig. 6a). During this period, the Golgi pattern of staining appeared in only a small number of cells. At the last stage of the culture, minimal extracellular signals were seen but they did not develop to a web-like accumulation (Fig. 6b).

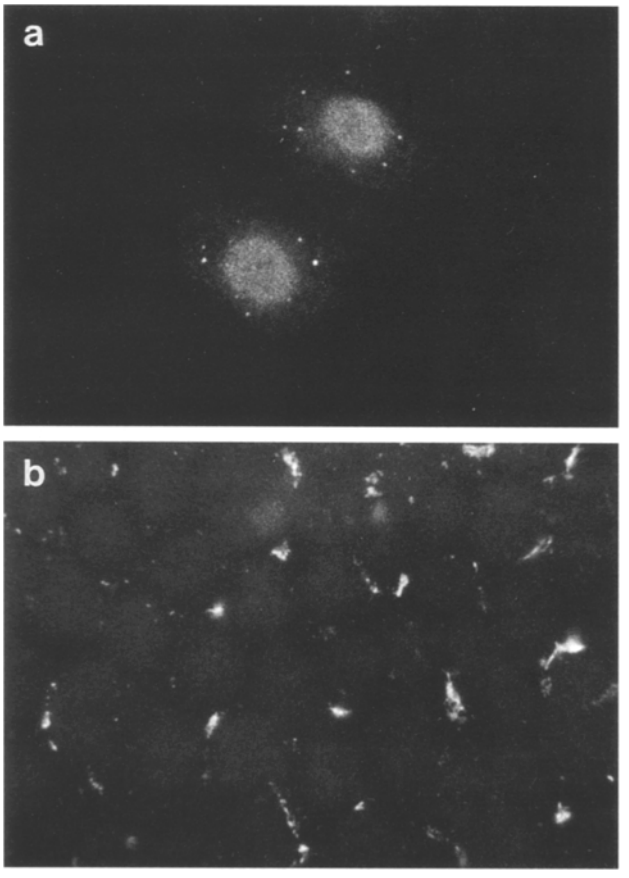

Fig. 6a, b Immunofluorescence for entactin in ACC3 cells. **a** Day 1, ×500. **b** Day 10, ×500. Both ER pattern signals (**a**) and intercellular deposits (**b**) are in less plentiful

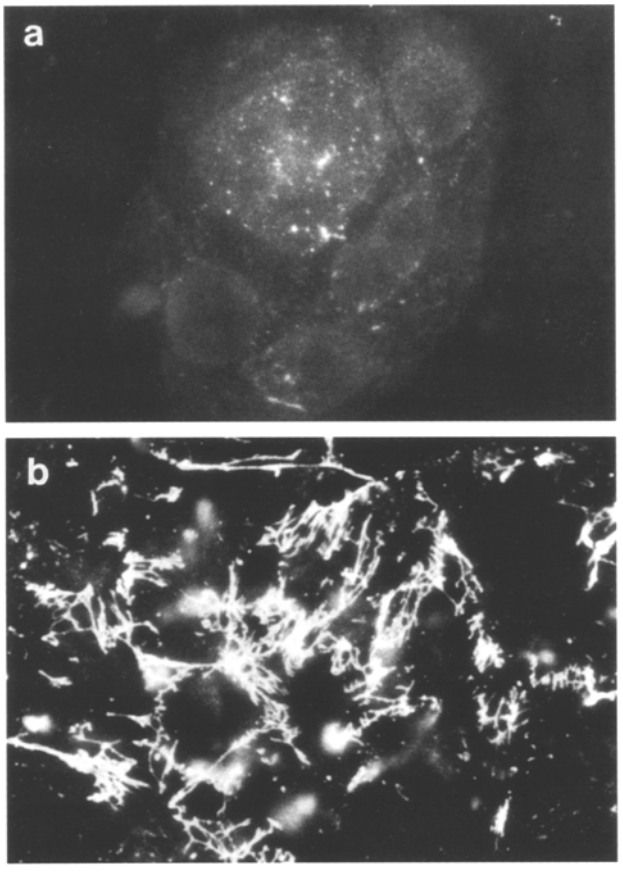

Fig. 7a, b Immunofluorescence for fibronectin in ACC3 cells. **a** Day 4, ×600. **b** Day 7, ×500. In contrast to its faint ER pattern (**a**), thick extracellular deposits (**b**) are characteristic of fibronectin

Fibronectin

Although similar results were obtained for fibronectin, extracellular deposits of fibronectin were the most conspicuous feature (Fig. 7b), in contrast to a rather faint ER pattern (Fig. 7a). Furthermore, remodelling of extracellular deposits and revival of Golgi pattern were noticeable.

Confocal immunofluorescence

Representative confocal images for signals of ER pattern, Golgi pattern, and extracellular deposits of extracellular matrix molecules examined, revealed no definite differences in X-Y axis slice images among the five molecules. Figure 8 shows four consecutive slices at Z axis of ACC3 cells immunostained for heparan sulphate proteoglycan at day 2. Fine granular signals of ER pattern were most concentrated at 4.8–6.4 μm from the cell base. Vertical reconstruction of X-Y axis slices showed that ER pattern signals were localized around the equatorial zone of a nucleus. Punctate signals of the Golgi pattern were more coarse and intensive than those of the ER pattern. Figure 9 shows that signals for laminin were localized around nuclei mainly at the equatorial zone (Fig. 9c; 5 μm from the cell base) and in the lower part of the cells (Figs. 9a, b; 3–4 μm from the cell base). The granular signals were in general divided by size, into ER and Golgi patterns. These two types of signal were both observed throughout the experimental course, although the ER pattern was predominant until day 3 and after that the Golgi pattern predominated until day 6.

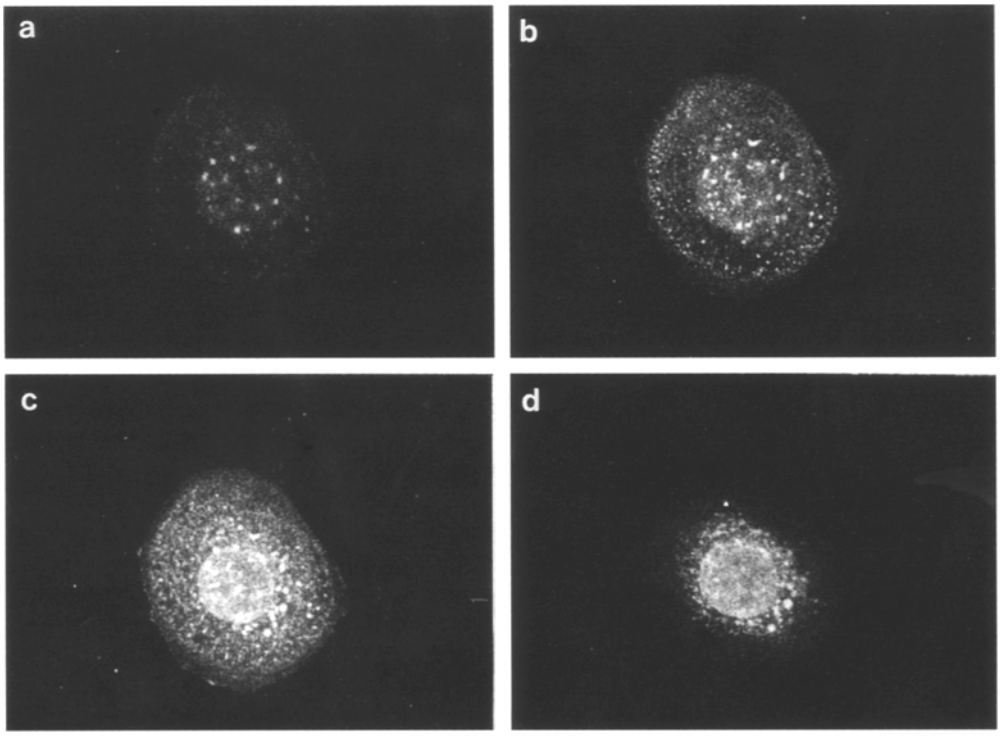

Fig. 8a–d Confocal images for HSPG immunolocalization in ACC3 cells, at day 2, showing ER pattern. Slices are arranged from cell base (**a**) to top (**d**). **a** 3.2 μm, **b** 4.8 μm, **c** 6.4 μm and **d** 8.0 μm from bottom of cell, ×560. ER pattern signals are condensed in equatorial zone of nucleus (**b**, **c**)

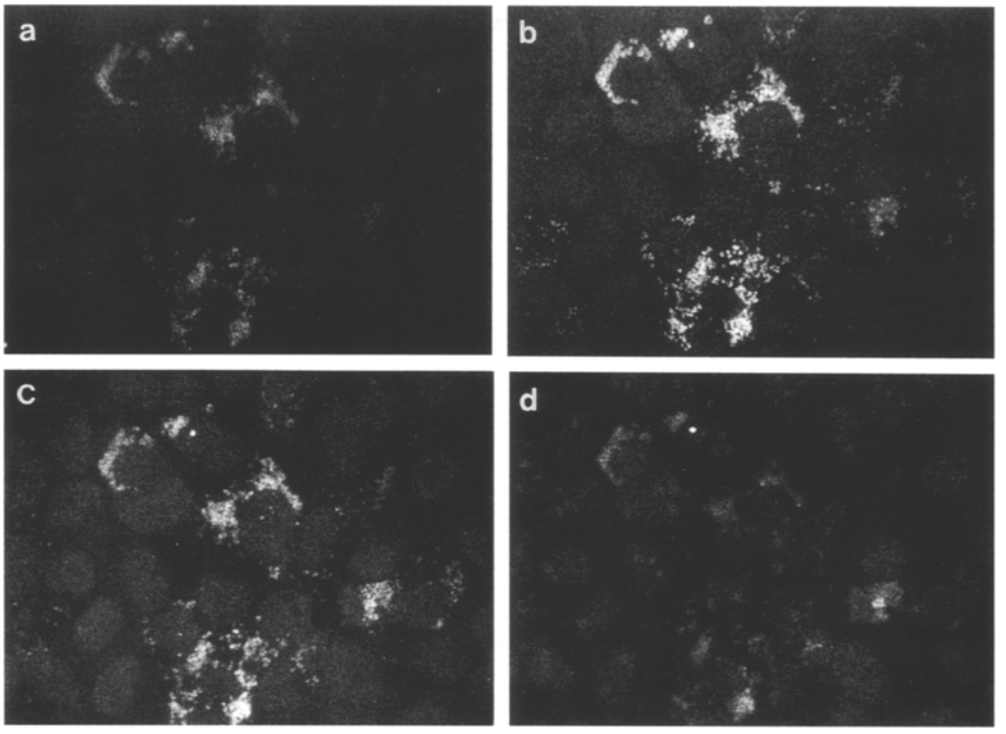

Fig. 9a–d Confocal images for laminin immunolocalization in ACC3, at day 5, showing Golgi patterns. **a** 3 μm, **b** 4 μm, **c** 5 μm and **d** 6 μm from cell base, ×570. Golgi pattern signals are localized around (**b**, **c**) or under (**a**) nuclear equatorial zones

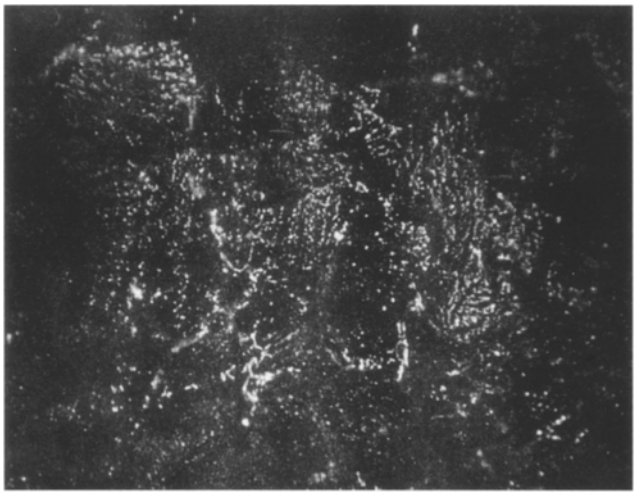

Fig. 10 Confocal images for fibronectin immunolocalization in ACC3 cells, at day 6, showing extracellular deposition in dotted or short linear fashion at basal surface of cells, ×460. Linear signals are generally paralleled in the same directions

When compared with conventional immunofluorescence, extracellular signals were more distinctly localized by this technique. In early stages, extracellular signals appeared on the basal surfaces of cells and were clearly detectable, as the confocal microscopy eliminated stratified cytoplasmic signals. Initially dotted signals changed gradually into straight or corrugated lines which were arranged in parallel. These linear signals sometimes showed a centripetal arrangement within each cell (Fig. 10). While the basal aspect of cells was extensively spread with a web of extracellular deposits (Fig. 11a), lateral or intercellular signals started to appear (Figs. 11b, c). They were accumulated nearly up to the apical surface of cells by the time of confluence (Fig. 11d). During the process of lateral and intercellular accumulation, fluorescence at the cell base decreased in area and in intensity.

Discussion

The present study has demonstrated the apparent biosynthesis of fibronectin and the four basement membrane molecules: type IV collagen, laminin, heparan sulphate proteoglycan and entactin by the parenchymal cells of ACC. The cell systems used in this study were established independently from different sources of human minor salivary gland and parotid gland [13]. However, there was no definite difference between the two in terms of proliferation profiles and productivity of extracellular matrix. The transplantation experiment indicated that these cells preserved their nature to form pseudocystic cavities, which were shown to contain the five extracellular matrix moieties immunohistochemically.

We have already shown that the pseudocysts characteristic of this type of carcinoma are filled with at least four constituent molecules of the basement membrane [10]. The present study shows evidence that the stromal accumulation of basement membrane molecules resulted from tumour cell secretion. This had been suggested in the previous electron microscopic studies, showing no cellular components but multiple layered basement membrane-like structures in the pseudocystic space [7, 9, 14, 15, 29].

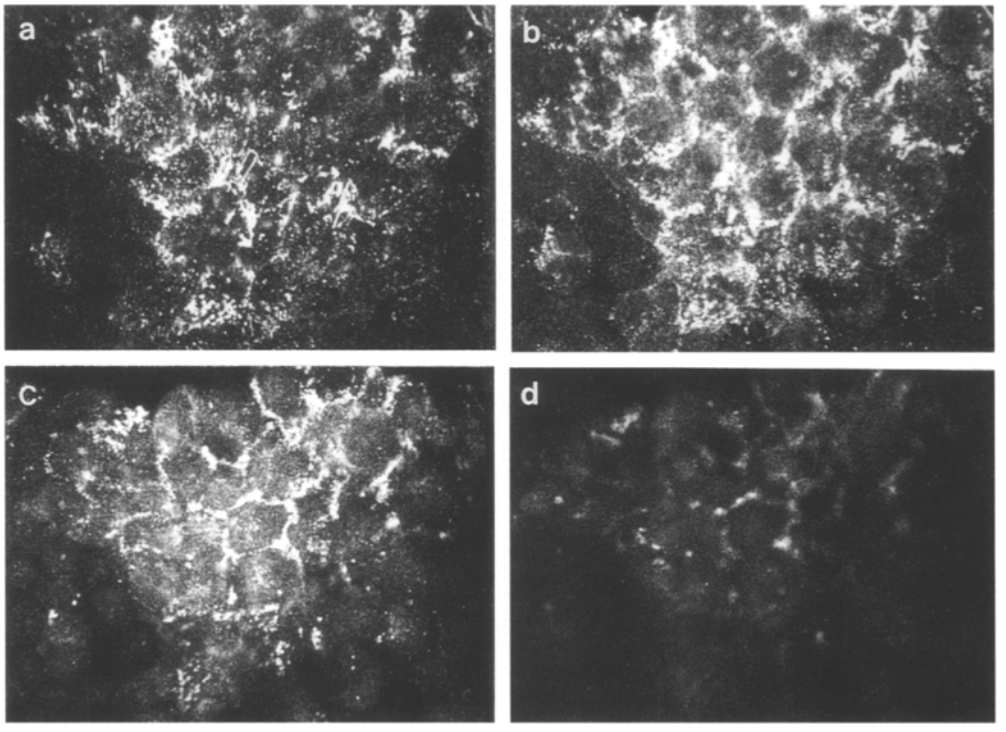

Fig. 11a–d Confocal images for fibronectin immunolocalization in ACC3 cells, at day 8, showing extracellular deposition in linear fashion at basolateral surface of cells. **a** 5.6 μm, **b** 7.2 μm, **c** 8.8 μm and **d** 10.4 μm from cell base, ×570. There are thick deposits of fibronectin at the lateral and intercellular space (**b**, **c**) as well as at the basal surface of cells (**a**). Intercellular signals are accumulated up to the level of the apical surface (**d**)

Production of basement membrane molecules by ACC has been suggested by the three previous experiments. One is the xenograft of ACC tissues into nude mice shown by Barsky et al. [2]. They demonstrated laminin and type IV collagen in the extracts of transplanted tumour tissues by enzyme-linked immunosorbent assay and sodium dodecyl sulphate polyacrylamide gel electrophoresis. Two others are immunohistochemical demonstrations in cell lines established from ACC of the human salivary gland. Sobue et al. [27] showed type IV collagen, laminin, fibronectin and chondroitin sulphate proteoglycan in the intercellular matrix and on the surface of the cells by the immunoperoxidase technique. Shirasuna et al. [25, 26] isolated two cell lines from two different ACCs. They showed that these cells had myoepithelial nature and potential for the production of fibronectin, laminin and type IV collagen. However, they merely showed immunoreactions for these molecules at a single section of culture and there has been no extensive investigation on the secretory pathway of those molecules in these cell systems. In the present study we were able to show direct evidence of biosynthesis of five extracellular molecules by the tumour cells, the process of intracellular transit and extracellular deposition of the molecules in the course of ACC2/ACC3 growth in culture.

Our time course study revealed that biosynthesis of the five molecules was first represented by the intracellular ER and Golgi patterns of immunofluorescence. The transition from intracellular signals to extracellular ones and the developing of extracellular signals from punctate or linear to meshwork patterns indicated that these molecules were secreted to the extracellular space by ACC2/ACC3 cells. The results suggest that a large part of the characteristic stroma of ACC is formed by the parenchymal cells, although ACC cells may change their phenotypic expression for these molecules significantly under culture conditions. Furthermore, it is still a matter of controversy whether the stromal cells take part in formation of the characteristic stroma.

Confocal microscopy is an essential tool for determing the intracellular localization of molecules [28]. It is even more powerful than electron microscopy for a chase study of secretory protein dynamics. The most attractive is three dimensional rearrangement of multiple Z-axis slice images. In the present study, we were able to localize granular signals for basement membrane molecules possibly in the rER and Golgi apparatus around the nuclear equatorial zone or in the lower space. This technique also enabled us to distinguish signals on the cell base from intracellular ones. The parallel arrangement of basal surface signals suggests that ACC cells left their traces of spreading and migration via focal contacts [34]. Based on these observations, we speculate that the extracellular matrix molecules are first secreted from the basal aspect of cell membranes for easier spreading and migration, followed by secretions from the lateral surface. These molecules seem to be synthesized and modified in the lower zone of the cell, that would not be inconsistent with their basolateral secretory pathways. Since we did not observe apical secretions of those molecules, cellular polarity might be organized in these cell systems. Heparan sulphate proteoglycans of basement membrane type have been shown to be contained in the culture media of bovine endothelial cells [22], mouse parietal yolk sac carcinoma PYS-2 cells [35] and mouse teratocarcinoma

HR9 cells [18], although their pathways of shedding into the media were unknown. The present result suggests that the lateral secretion, but not apical, would be a possibility for those cells in monolayer cultures.

It has been well documented that extracellular matrices including basement membrane constituent molecules have potential to promote cellular growth or differentiation, and organogenesis [31]. In the present study, an accelerated growth of ACC2 and ACC3 cells was confirmed by the presence of fibronectin, especially in the early stages of culture. The decline of their growth curves seems to be in concordance with extracellular accumulation of the five molecules by their own secretion. Lateral and intercellular association with extracellular matrix molecules might not benefit growth these cells in a monolayer culture. Anyhow, we consider that ACC2 and ACC3 cells are valuable cell systems for various kinds of extracellular matrix studies.

Recent advances in the basement membrane study have owed a great deal to the mouse (Engelbreth-Holm-Swarm) (EHS) tumour [21, 31]. Most of the basement membrane molecules were isolated from this tumour and then characterized [3, 5, 12, 24] and EHS tumour-derived specimens have been supplied for sources of biological experiments and as antigens for raising antibodies. Recently, significant difference in molecular structures were found between the human heparan sulphate proteoglycan core protein and the murine EHS derived one [16, 20], although it is unknown whether such differences between species play an important role in in vitro experimentation. The present results suggest that our cell lines are good sources of human basement membrane components, as there have been no other basement membrane producing cell systems of human origin available for the present. Barsky et al. [2] showed that the yields of laminin and type IV collagen from ACC xenografts in nude mice was 16% and 18% (mg protein/g tumour), respectively, of EHS tumours.

Since the information obtained here is based only on light microscopic immunohistochemistry for fibronectin and basement membrane proteins, we need more investigation of their immunolocalization at electron microscopic level and of gene expression before the complete pathways of these molecules from intracellular transport to extracellular deposition is made clear.

Acknowledgements We wish to thank Dr. Hidehiro Ozawa, Niigata University School of Dentistry, for his generous allowance for our laser scanning microscopic study in his laboratory. This work is supported by grants-in-aid for scientific research from the Ministry of Education, Science and Culture, Japan and from the Niigata University Science Foundation.

References

1. Azumi N, Battifora H (1987) The cellular composition of adenoid cystic carcinoma. An immunohistochemical study. Cancer 60:1589–1598
2. Barsky SH, Layfield L, Varki N, Bhuta A (1988) Two human tumors with high basement membrane-producing potential. Cancer 61:1798–1806
3. Bornstein P, Sage H (1980) Structurally distinct collagen types. Annu Rev Biochem 49:957–1003
4. Busuttil A (1977) Adenoid cystic carcinoma of the minor salivary glands. J Laryngol Otol 91:41–53
5. Carlin B, Jaffe R, Bender B, Chung AE (1981) Entactin, a novel basal lamina-associated sulfated glycoprotein. J Biol Chem 256:5209–5214
6. Caselitz J, Schulze I, Seifert G (1986) Adenoid cystic carcinoma of the salivary glands: an immunohistochemical study. J Oral Pathol Med 15:308–318
7. Chen SY (1976) Adenoid cystic carcinoma of minor salivary gland. Histochemical and electron microscopic studies of cyst-like spaces. Oral Surg Oral Med Oral Pathol 42:606–619
8. Cheng J, Liu AR, Liu Z (1985) A clinicopathological study of 225 cases of adenoid cystic carcinoma of salivary glands. Chin J Stomatol 20:15–18
9. Cheng J, Liu AR, Liu Z (1985) Electron microscopic and histochemical study of adenoid cystic carcinoma of salivary gland. Chin J Stomatol 20:135–137
10. Cheng J, Saku T, Okabe H, Furthmayr H (1992) Basement membranes in adenoid cystic carcinoma: an immunohistochemical study. Cancer 69:2631–2640
11. Engvall E, Ruoslahti E (1977) Binding of soluble form of fibroblast surface protein, fibronectin, to collagen. Int J Cancer 20:1–5
12. Fujiwara S, Wiedemann H, Timpl R, Lustig A, Engel J (1984) Structure and interactions of heparan sulfate proteoglycans from a mouse tumor basement membrane. Eur J Biochem 1443:145–157
13. He RG, Zhang XS, Zhou XJ, Wang Z, Zhang XL, Qiu WL, Han YS, Zhang RX (1988) The establishment of cell lines of adenoid cystic carcinoma of human salivary glands (ACC2, ACC3) and a study of morphology. West Chin J Stomatol 6:1–4
14. Hoshino M, Yamamoto I (1970) Ultrastructure of adenoid cystic carcinoma. Cancer 25:186–198
15. Hübner G, Kleinsasser O, Klein H (1969) Zur Feinstruktur und Genese der Cylindrome der Speicheldrüsen. Virchows Arch [A] 347:296–315
16. Kallunki P, Tryggvason K (1992) Human basement membrane heparan sulfate proteoglycan core protein: a 467-kD protein containing multiple domains resembling elements of the low density lipoprotein receptor, laminin, neural cell adhesion molecules, and epidermal growth factor. J Cell Biol 116:559–571
17. Katsuta H, Takaoka T, Oishi Y, Baba T, Chang KC (1954) Cultivation of fibroblasts from chick embryo heart in the simplified replicate tissue culture. Jpn J Exp Med 24:125–139
18. Keller R, Furthmayr H (1986) Isolation and characterization of basement membrane and cell proteoheparan sulphates from HR9 cells. Eur J Biochem 161:707–714
19. Nochomovitz LE, Kahn LB (1977) Adenoid cystic carcinoma of the salivary gland and its histologic variants. Oral Surg Oral Med Oral Pathol 44:394–404
20. Noonan DM, Horigan EA, Ledbetter SR, Vogeli G, Sasaki M, Yamada Y, Hassell JR (1988) Identification of cDNA clones encoding different domains of the basement membrane heparan sulfate proteoglycan. J Biol Chem 263:16379–16387
21. Orkin RW, Gehron P, McGoodwin EB, Martin GR, Valentine T, Swarm R (1977) A murine tumor producing a matrix of basement membrane. J Exp Med 145:204–220
22. Saku T, Furthmayr H (1989) Characterization of the major heparan sulfate proteoglycan secreted by bovine aortic endothelial cells in culture: Homology to the large molecular weight molecule of basement membrane. J Biol Chem 265:3514–3523
23. Saku T, Okabe H, Yagi Y, Sato E, Tsuda N (1984) A comparative study on the immunolocalization of keratin and myosin in salivary gland tumors. Acta Pathol Jpn 41:1031–1040
24. Sasaki M, Kleinmann HK, Huber H, Deutzmann R, Yamada Y (1988) Laminin, a multidomain protein. The A chain has a unique globular domain and homology with the basement

membrane proteoglycan and the laminin B chains. J Biol Chem 263:16536–16544
25. Shirasuna K, Watatani K, Furusawa H, Saka M, Morioka S, Yoshioka H, Matsuya T (1990) Biological characterization of pseudocyst-forming cell lines from human adenoid cystic carcinomas of minor salivary gland origin. Cancer Res 50:4139–4145
26. Shirasuna K, Saka M, Hayashido Y, Yoshioka H, Sugiura T, Matsuya T (1993) Extracellular matrix production and degradation by adenoid cystic carcinoma cells: participation of plasminogen activator and its inhibitor in matrix degradation. Cancer Res 53:147–152
27. Sobue M, Takeuchi J, Niwa M, Yasui C, Nakagaki S, Nagasaka T, Fukatsu T, Saga A, Nakashima N (1989) Establishment of a cell line producing basement membrane components from an adenoid cystic carcinoma of the human salivary gland. Virchows Arch [B] 57:203–208
28. Takamatsu T, Fujita S (1988) Microscopic tomography by laser scanning microscopy and its three-dimensional reconstruction. J Microsc 149:167–174
29. Tandler B (1971) Ultrastructure of adenoid cystic carcinoma of salivary gland origin. Lab Invest 24:504–512
30. Thackray AC, Lucas RB (1974) Tumor of the major salivary glands. Armed Forces Institute of Pathology, Washington, DC, pp 91–99
31. Timpl T (1989) Structure and biological activity of basement membrane proteins. Eur J Biochem 180:487–502
32. Toida M, Takeuchi J, Hara K, Sobue M, Tsukidate K, Goto K, Nakashima N (1984) Histochemical studies of intercellular components of salivary gland tumors with special reference to glycosaminoglycan, laminin and vascular elements. Virchows Arch [A] 403:15–26
33. Toida M, Takeuchi J, Sobue M, Tsukidate K, Akao S, Fukatsu T, Nakashima N (1985) Histochemical studies on pseudocysts in adenoid cystic carcinoma of the human salivary gland. Histochem J 17:913–924
34. Turner CE, Burridge K (1991) Transmembrane molecular assemblies in cell-extracellular matrix interactions. Curr Opin Cell Biol 3:849–853
35. Tyree B, Horigan EA, Klippenstein DL, Hassell JR (1984) Heterogeneity of heparan sulfate proteoglycans synthesized by PYS-2 cells. Arch Biochem Biophys 231:328–335